© 2014. Published by The Company of Biologists Ltd | Journal of Cell Science (2014) 127, 4368–4380 doi:10.1242/jcs.145912

RESEARCH ARTICLE

Histone acetylation in astrocytes suppresses GFAP and stimulates a reorganization of the intermediate filament network

Regina Kanski[1], Marjolein A. M. Sneeboer[1], Emma J. van Bodegraven[1], Jacqueline A. Sluijs[1], Wietske Kropff[1], Marit W. Vermunt[2], Menno P. Creyghton[2], Lidia De Filippis[3], Angelo Vescovi[3,4], Eleonora Aronica[5,6,7], Paula van Tijn[1,8], Miriam E. van Strien[1] and Elly M. Hol[1,7,9,*]

ABSTRACT

Glial fibrillary acidic protein (GFAP) is the main intermediate filament in astrocytes and is regulated by epigenetic mechanisms during development. We demonstrate that histone acetylation also controls GFAP expression in mature astrocytes. Inhibition of histone deacetylases (HDACs) with trichostatin A or sodium butyrate reduced *GFAP* expression in primary human astrocytes and astrocytoma cells. Because splicing occurs co-transcriptionally, we investigated whether histone acetylation changes the ratio between the canonical isoform *GFAPα* and the alternative *GFAPδ* splice variant. We observed that decreased transcription of *GFAP* enhanced alternative isoform expression, as HDAC inhibition increased the *GFAPδ*:*GFAPα* ratio. Expression of *GFAPδ* was dependent on the presence and binding of splicing factors of the SR protein family. Inhibition of HDAC activity also resulted in aggregation of the GFAP network, reminiscent of our previous findings of a GFAPδ-induced network collapse. Taken together, our data demonstrate that HDAC inhibition results in changes in transcription, splicing and organization of GFAP. These data imply that a tight regulation of histone acetylation in astrocytes is essential, because dysregulation of gene expression causes the aggregation of GFAP, a hallmark of human diseases like Alexander's disease.

KEY WORDS: Astrocytes, Neural stem cells, Alternative splicing, Epigenetics, GFAP isoforms

INTRODUCTION

In the adult mammalian brain, astrocytes represent the major population of glial cells. Astrocytes are crucial for neuronal support, including synaptic transmission and information processing by neural circuits. They maintain central nervous system homeostasis by regulating ion concentrations, metabolizing neurotransmitters and by controlling cerebral blood flow. Moreover, astrocytes vigorously react to brain damage or disease and they have neurogenic properties in specific brain niches (Sofroniew and Vinters, 2010). The main intermediate filament protein in astrocytes is glial fibrillary acidic protein (GFAP), a type III intermediate filament, which is widely used as a signature protein for astrocytes. Upregulation of GFAP is a hallmark of reactive astrocytes in the diseased brain (Middeldorp and Hol, 2011). In line with a function of GFAP in reactive gliosis, GFAP-knockout mice are more sensitive to injury such as cervical spinal cord injury, cerebral ischemia or mechanical trauma (Nawashiro et al., 1998; Nawashiro et al., 2000; Otani et al., 2006; Wilhelmsson et al., 2004; de Pablo et al., 2013). Overexpression of GFAP in mice results in death a few weeks after birth (Messing et al., 1998), partially resembling Alexander's disease (AxD), a fatal human neurodegenerative disease (Alexander, 1949). In AxD, mutations in the *GFAP* gene result in elevated GFAP expression, indicating gain-of-function mutations (Hagemann et al., 2005; Tian et al., 2006).

The *GFAP* gene is alternatively spliced and, to date, ten different isoforms have been discovered in the human brain. The canonical isoform is GFAPα, and the most abundant alternatively spliced variant is GFAPδ (Middeldorp and Hol, 2011). In the healthy brain, GFAPα is expressed in grey and white matter astrocytes, subpial astrocytes and neurogenic astrocytes along the ventricles, whereas GFAPδ is expressed at a lower level and is mainly present in subpial astrocytes and in the subventricular zone neurogenic astrocytes. GFAPδ expression is induced in reactive astrocytes in the diseased brain as described in patients with epilepsy, Alzheimer disease and gliomas (Martinian et al., 2009; Roelofs et al., 2005; Andreiuolo et al., 2009; Choi et al., 2009).

Expression levels of *GFAP* are controlled by the activity of the GFAP promoter, a process that is highly dependent on epigenetic modifications. During the initiation of astrogenesis in neural stem cells (NSCs), demethylation of the *GFAP* promoter activates transcription of *GFAP* (Kanski et al., 2014; Takizawa et al., 2001; Fan et al., 2005; Namihira et al., 2009). Moreover, histone acetylation has been shown to control GFAP expression in differentiating NSCs dependent on the developmental state of the cell (Hsieh et al., 2004; Asano et al., 2009; Zhou et al., 2011). The acetylation state of histone proteins is regulated by histone acetylase and histone deacetylase (HDAC) enzymes.

The recruitment of splicing factors occurs during the process of pre-mRNA transcription. Thus, transcriptional regulators such as

[1]Astrocyte Biology & Neurodegeneration, Netherlands Institute for Neuroscience, An Institute of the Royal Netherlands Academy of Arts and Sciences, Meibergdreef 47, 1105 BA Amsterdam, The Netherlands. [2]Hubrecht Institute-KNAW & University Medical Center Utrecht, Uppsalalaan 8, 3584CT, Utrecht, The Netherlands. [3]Department of Biotechnologies, Fondazione Centro San Raffaele del Monte Tabor, 20132 Milan, Italy. [4]Ospedale Casa Sollievo della Sofferenza, 71013 San Giovanni Rotondo (FG), Italy. [5]Department of Neuropathology, Academic Medical Center, University of Amsterdam (UvA), 1105 AZ Amsterdam, The Netherlands. [6]SEIN – Stichting Epilepsie Instellingen Nederland, 2103 SW Heemstede, The Netherlands. [7]Swammerdam Institute for Life Sciences, Center for Neuroscience, University of Amsterdam, 1090 GE Amsterdam, The Netherlands. [8]Hubrecht Institute, an Institute of the Royal Netherlands Academy of Arts and Sciences and University Medical Centre Utrecht, 3508 AD Utrecht, The Netherlands. [9]Department of Translational Neuroscience, Brain Center Rudolf Magus, University Medical Center Utrecht, Universiteitsweg 100, 3584 CX, Utrecht, The Netherlands.

*Author for correspondence (e.m.hol-2@umcutrecht.nl)

Received 8 November 2013; Accepted 20 July 2014

Journal of Cell Science

Journal of Cell Science (2014) 127, 4368–4380 doi:10.1242/jcs.145912

HDACs can potentially affect the splicing process (Zhou et al., 2012; Kornblihtt et al., 2004; Luco et al., 2010). Histone acetylation determines the chromatin status of a gene, which influences the transcription rate of RNA polymerase II (RNA pol II). Classically, histone acetylation is associated with an open chromatin structure and increased binding of transcriptional activators. However, expression levels of numerous genes have been shown to be decreased upon HDAC inhibition, in contrast to the classical view (Hnilicová et al., 2011).

The RNA pol II complex is often seen as the direct link between transcription and the splicing process. In the case of a fast elongation rate of the polymerase, there might not be enough time for the recruitment of splicing factors to imperfect (weak) splice sites of the alternative exons, because both strong splice sites (encoded by constitutive exons) and weaker splicing sites (encoded by alternative exons) compete for the recruitment of the same splicing factors (Wahl et al., 2009). Hence, fast transcription results in the skipping of alternative exons and a reduction in the amount of alternatively spliced mRNAs. At a slow elongation rate of the RNA polymerase, all exons are recognized by the splicing factors and thus are included in the transcript, which allows for enhanced expression of alternative transcripts (Hnilicová et al., 2011; Kornblihtt et al., 2004). The splicing factors of the SR protein family are key activators of constitutive as well as alternative splicing. The availability and binding of SR proteins regulates the recognition and inclusion of exons (Long and Caceres, 2009).

The alternative *GFAPδ* transcript is generated by recognition of imperfect splice sites in an alternative exon located in the seventh intron, termed ‘exon 7+’ (Blechingberg et al., 2007). The alternative exon replaces the classical exons 8 and 9 at the 3′ end of the *GFAP* transcript (Nielsen et al., 2002). Exon 7+ is highly conserved across species (Boyd et al., 2012) and encodes an alternative C-terminal tail, which compromises the assembly of GFAP filaments. For proper filament formation, GFAPδ requires the presence of GFAPα protein (Perng et al., 2008; Roelofs et al., 2005). This implies that a tight regulation of *GFAP* splicing is important to ensure a balanced ratio of GFAPδ:GFAPα and, in turn, optimal GFAP network assembly. In intermediate-filament-free cells, it has been shown that a GFAPδ:GFAPα ratio of 1:3 is necessary for proper network formation (Kamphuis et al., 2012; Nielsen et al., 2002). Expression of GFAPδ at higher concentrations induces a collapse of the GFAP filament network around the nucleus (Roelofs et al., 2005; Nielsen et al., 2002; Perng et al., 2008). Based on the increasing evidence of an interplay between transcription and alternative splicing, we hypothesized that suppression of histone deacetylation would not only regulate *GFAP* expression but also would affect the alternative splicing of *GFAP* transcripts and modulate GFAP network assembly.

RESULTS

Histone acetylation in astrocytes reduces *GFAP* expression and alters the isoform usage

The aim of this study was to investigate whether *GFAP* expression levels in general, and *GFAP* isoform expression in particular, is regulated by histone acetylation in human astrocytes. To this end, histone deacetylation was suppressed using two different histone deacetylase inhibitors (HDACi). The effect of HDACi treatment on the two most abundant *GFAP* isoforms – the canonical *GFAP* isoform *GFAPα* and the alternatively spliced form *GFAPδ* – was first investigated in primary human astrocytes. The cells were treated for 24 hours with the HDACi trichostatin A (TSA, 660 nM). HDAC inhibition with TSA induced a downregulation of *GFAPα* and a trend towards decreased *GFAPδ* expression. Owing to a more pronounced reduction of *GFAPα* than *GFAPδ* expression, the *GFAPδ*:*GFAPα* ratio significantly increased (Fig. 1A). In order to emphasize a relative increase in the contribution of the assembly-compromised splice-variant *GFAPδ* to total GFAP levels, we chose to display the *GFAPδ*:*GFAPα* ratio throughout the manuscript. Next, we explored whether U343 astrocytoma cells represent a suitable cell model to further investigate the effect of histone acetylation on *GFAP* expression, because human primary astrocytes are of limited availability and are prone to loss of their *GFAP* expression at higher passages (Gibbons et al., 2007). HDAC inhibition with TSA significantly decreased the expression of *GFAPα* and *GFAPδ* in U343 cells. As in primary cells, a more pronounced reduction of *GFAPα* in comparison to *GFAPδ* expression led to an increase in the *GFAPδ*:*GFAPα* ratio (Fig. 1B). Treatment with an alternative HDACi, sodium butyrate (5 mM), also resulted in a trend towards reduced expression of *GFAPα*, *GFAPδ* and an increase in the *GFAPδ*:*GFAPα* ratio in primary human astrocytes (Fig. 1C). HDAC inhibition with sodium butyrate in U343 cells resulted in significantly reduced expression levels of *GFAPα*, *GFAPδ* and an increase in the *GFAPδ*:*GFAPα* ratio (Fig. 1D). Similar concentrations of these inhibitors have been previously found to modulate alternative splicing of genes in non-astrocytic cell lines (Puppin et al., 2011; Hnilicová et al., 2011). These data demonstrate that suppression of histone deacetylation in astrocytes decreases GFAP transcription and increases the *GFAPδ*:*GFAPα* ratio in favor of the alternatively spliced form *GFAPδ*. To control for the efficacy of the HDAC inhibition, the expression of *HDAC3* and *jun* mRNA was determined. A compensatory upregulation of *HDAC3* expression has been described upon efficient HDAC inhibition (Ajamian et al., 2004; Dangond and Gullans, 1998). Moreover, sodium butyrate treatment was shown to induce expression of the *jun* oncogene (Hnilicová et al., 2011). Consistently, treatment of U343 cells with TSA upregulated *HDAC3* expression, whereas sodium butyrate significantly induced *HDAC3* as well as *jun* expression (Fig. 1E,F).

Taken together, we demonstrate here that suppression of histone deacetylation using two different inhibitors decreases *GFAP* expression and alters the *GFAP* isoform usage in primary human astrocytes (Fig. 1A,C) and in astrocytoma cells (Fig. 1B,D). These data show that histone deacetylation is fundamentally involved in regulating *GFAP* mRNA levels and *GFAP* isoform expression in astrocytes.

In order to investigate the effect of HDAC inhibition on histone acetylation at the *GFAP* promoter, we performed a chromatin immunoprecipitation using an antibody against acetylated lysine 27 of histone 3 (H3K27ac). In cells treated for 24 hours with 2 or 5 mM sodium butyrate, H3K27 acetylation at the *GFAP* promoter was reduced in comparison to that of DMSO-treated cells (Fig. 2A). The transcriptional start site (TSS) itself is a histone-free region and therefore H3K27 acetylation was investigated 500 base pairs upstream of the TSS. H3K27 acetylation at intragenic sequences of the *GFAP* gene remained unchanged upon HDAC inhibition (data not shown). An increase in H3K27 acetylation has been previously linked to an open chromatin structure at the *GFAP* promoter and active *GFAP* transcription (Cheng et al., 2011). Consistently, here, we show that reduced H3K27 acetylation at the *GFAP* promoter is linked to reduced *GFAP* expression. This finding is in line with previous reports of

Journal of Cell Science (2014) 127, 4368–4380 doi:10.1242/jcs.145912

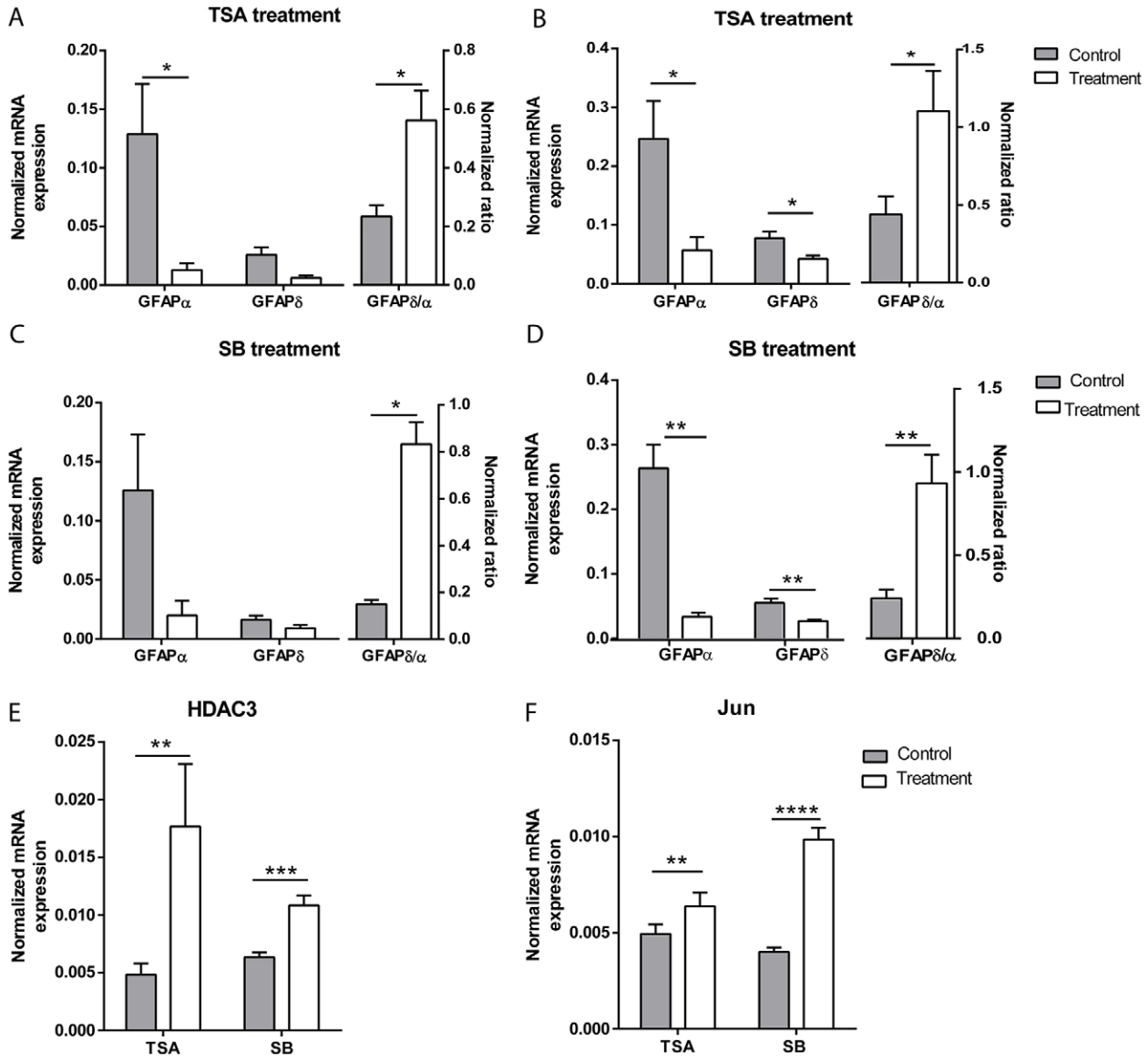

Fig. 1. Suppression of histone deacetylation reduces *GFAP* expression and alters its isoform usage in astrocytic cells. Quantitative (q)PCR analysis of the *GFAPα* and *GFAPδ* transcripts upon treatment of primary human astrocytes with (A) TSA (660 nM), (C) sodium butyrate (SB, 5 mM) or vehicle for 24 hours (n=4). The *GFAPδ*:*GFAPα* ratio is also shown. (B,D) Expression analysis of the *GFAPα* and *GFAPδ* transcripts in U343 cells upon treatment with TSA (B), sodium butyrate (D) or vehicle for 24 hours (n=6). Expression of HDAC3 (E) as well as the jun (Jun) oncogene (F) is increased upon treatment with sodium butyrate or TSA. Data were normalized to the reference genes actin and 18S and are presented as the mean+s.e.m. *P<0.05, **P<0.01, ***P<0.001, ****P<0.0001.

deacetylation of the promoters of genes downregulated by HDACi (Rada-Iglesias et al., 2007, Duan et al., 2005; Reid et al., 2005). In contrast to the regional decrease in H3K27 acetylation at the *GFAP* promoter, global histone acetylation upon HDAC inhibition was increased in U343 cells. As expected, treatment with the HDACi sodium butyrate increased H3K27 acetylation in a dose-dependent manner (Fig. 2B). We also determined increased H3K27 acetylation in the 45S pre-ribosomal gene, and a lack of H3K27 acetylation in an area devoid of genes using chromatin immunoprecipitation (data not shown; primer sequences named 18S and GD1, respectively, in supplementary material Table S1). Taken together, our chromatin immunoprecipitation and western blotting data on H3K27 acetylation show (1) a decrease in histone acetylation at the GFAP promoter and (2) a global increase in histone acetylation levels in HDACi-treated cells.

HDAC inhibition induces a reorganization of the intermediate filament network of astrocytes

Subsequently, we analyzed whether an increase in the *GFAPδ*:*GFAPα* ratio translates into changes in the GFAP protein network. Previously, it has been demonstrated that the ratio of GFAPδ:GFAPα is an important determinant of the GFAP network assembly – a shift towards higher GFAPδ expression induces aggregation of the GFAP filament network (Perng et al., 2008; Nielsen et al., 2002; Roelofs et al., 2005). In order to investigate whether changes in mRNA levels of GFAP translate into changes in protein levels, we performed western blotting

Journal of Cell Science (2014) 127, 4368–4380 doi:10.1242/jcs.145912

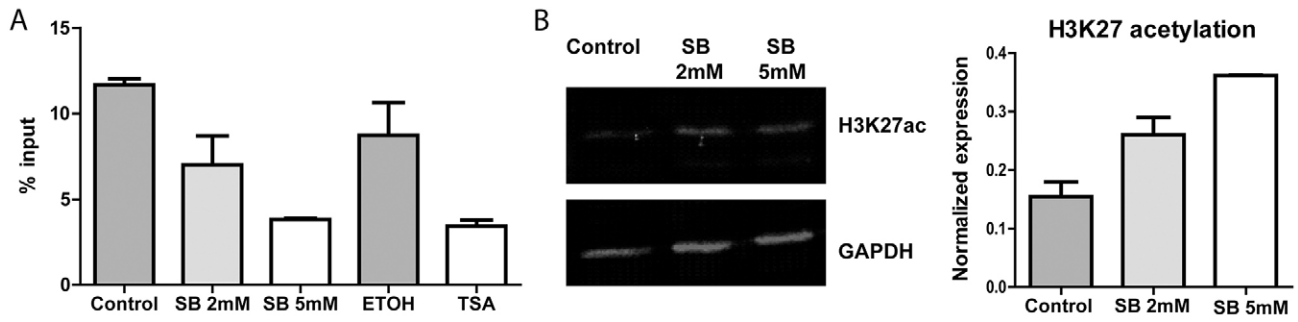

Fig. 2. HDAC inhibition reduces H3K27 acetylation at the *GFAP* promoter and increases global H3K27 acetylation levels in U343 cells. (A) Chromatin immunoprecipitation-qPCR analysis of U343 cells treated for 24 hours with vehicle (Control), sodium butyrate (SB, 2 or 5 mM) or TSA (660 nM). HDAC inhibition induced a decrease in H3K27 acetylation at 500 base pairs upstream of the transcriptional start site (TSS) of the *GFAP* gene (n=2, two independent experiments). ETOH, ethanol. (B) Left, western blot analysis of U343 cells treated for 72 hours with vehicle (Control) or 2 or 5 mM sodium butyrate. Right, quantification of H3K27 acetylation levels normalized to GAPDH revealed a dose-dependent increase of H3K27 acetylation upon treatment with sodium butyrate (n=2, two independent experiments). Quantitative data show the mean+s.e.m.

analysis of the different GFAP isoforms. In line with a downregulation of *GFAPα* and *GFAPδ* mRNA expression, protein levels of the GFAP isoforms were reduced upon HDAC inhibition. A more pronounced reduction of GFAPα than GFAPδ expression resulted in an increased GFAPδ:GFAPα ratio (Fig. 3A). To investigate whether the increased GFAPδ:GFAPα ratio induced by HDAC inhibition triggers a reorganization of the GFAP network, U343 cells were stained for pan-GFAP and GFAPδ after treatment with sodium butyrate for 24, 48 and 72 hours. No obvious changes in the GFAP network were observed after 24 and 48 hours (data not shown). However, cells treated with sodium butyrate for 72 hours showed an aggregation of the GFAP network in close proximity to the nucleus. Staining with an antibody against pan-GFAP, as well as a GFAPδ-specific antibody, showed a drastic redistribution of the GFAP network in comparison to that of control cells (Fig. 3B).

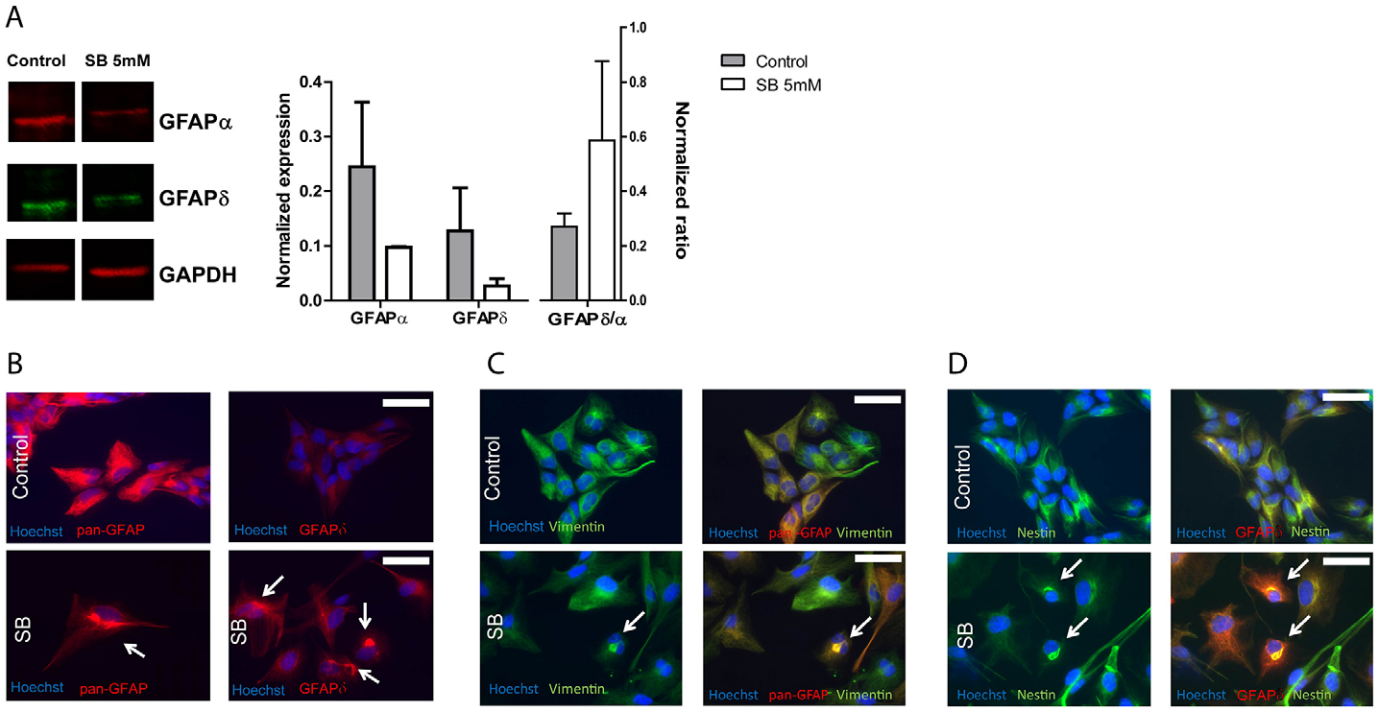

Fig. 3. HDAC inhibition reduces GFAP protein expression and induces a reorganization of the intermediate filament network. (A) Western blot analysis of DMSO-treated cells (Control) and sodium butyrate (SB)-treated cells (5 mM) revealed a downregulation of GFAPα and GFAPδ expression upon HDAC inhibition (left). Quantification of the GFAP expression normalized to GAPDH revealed a more pronounced reduction of GFAPα than GFAPδ expression, resulting in an increased GFAPδ:GFAPα ratio (right). Data show the mean+s.e.m. (B–D) The intermediate filament network of GFAP, vimentin and nestin is redistributed upon treatment with the HDACi sodium butyrate. (B) U343 cells were stained with an antibody against pan-GFAP or a GFAPδ-specific antibody together with the DNA stain Hoechst 33258. Sodium butyrate treatment for 72 hours induced a drastic redistribution of the GFAP network, which aggregated in close proximity to the nucleus. Arrows indicate cells with a reorganized intermediate filament network. (C) Vimentin staining together with staining of pan-GFAP revealed that vimentin coaggregates with GFAP in the sodium-butyrate-treated condition. (D) The nestin network is reorganized into aggregates where it colocalizes with GFAPδ. Scale bars: 50 μm.

Journal of Cell Science (2014) 127, 4368–4380 doi:10.1242/jcs.145912

The GFAP network is an integral component of the intermediate filament network in astrocytes, which consists of GFAP, vimentin, nestin and synemin (Jing et al., 2007). In order to investigate whether HDAC inhibition affects the organization of the whole intermediate filament network, we analyzed the localization of vimentin, nestin and synemin in cells treated with sodium butyrate. Importantly, vimentin staining in cells treated for 72 hours with sodium butyrate revealed an aggregation of vimentin together with GFAP in aggregates next to the nucleus. Cells under control conditions showed a normal intermediate filament network (Fig. 3C). In addition, the nestin network also aggregated together with GFAP in sodium-butyrate-treated cells, whereas a normal intermediate filament network was present in the control cells (Fig. 3D). Synemin expression was undetectable (data not shown). These data demonstrate that HDAC inhibition with sodium butyrate not only led to an increase in the GFAPδ:GFAPα ratio but subsequently led to a reorganization of the whole intermediate filament network of astrocytes.

HDAC inhibition is known to trigger apoptosis in a time-dependent manner (Svechnikova et al., 2008). To investigate whether the observed aggregate formation was linked to cell death, we performed staining for cleaved caspase 3 and propidium iodide staining of DNA. No apoptosis was detected after treatment with sodium butyrate for 72 hours, when the aggregate formation was observed. The absence of apoptotic cells at this time-point indicates that the observed aggregate formation is not caused by cell death. However, as expected, long-term treatment with sodium butyrate (e.g. for 5 days) did induce apoptosis as shown by cleaved caspase 3 staining and DNA staining with propidium iodide (supplementary material Fig. S1).

In order to confirm a role for HDACs in the observed aggregation of GFAP, we performed an RNA interference (RNAi) experiment targeting two different HDACs, namely HDAC3 and HDAC6. In line with a crucial role for HDACs in GFAP filament assembly, in cells with downregulation of either HDAC3 or HDAC6 expression, mediated by the expression of a specific small interfering RNA (siRNA), an aggregation of the GFAP network was observed (Fig. 4A). This reorganization of the GFAP network resembled the GFAP aggregation upon treatment with sodium butyrate. In cells treated with a control siRNA (NTC), no aggregation of the GFAP network was observed. Consistent with a reorganization of the GFAP filaments, *GFAP* mRNA expression in HDAC3-knockdown and HDAC6-knockdown cells is changed in comparison to that of control cells (Fig. 4B). Taken together, data derived from inhibition of HDAC activity by sodium butyrate (Fig. 3), as well as from knockdown of two different HDACs (Fig. 4), shows that the activity and expression of HDACs regulates the mRNA expression and filament assembly of GFAP.

A low concentration of sodium butyrate stimulates alternative splicing of *GFAP*

An increase in the *GFAPδ*:*GFAPα* ratio at the transcript level indicates enhanced alternative splicing of *GFAP*. Interestingly, we observed that treatment of U343 cells with 2 mM sodium butyrate led to an increase in the *GFAPδ*:*GFAPα* ratio but, in contrast to 5 mM sodium butyrate, this effect was solely due to an increase in the alternatively spliced isoform *GFAPδ*, as the *GFAPα* expression level remained unchanged (Fig. 5A). Similar to cells with an increased *GFAPδ*:*GFAPα* ratio upon treatment with 5 mM sodium butyrate, an increased *GFAPδ*:*GFAPα* ratio in cells treated with 2 mM sodium butyrate resulted in an aggregation of the GFAP filaments (supplementary material Fig. S2). An elevated *GFAPδ* expression indicates a stimulation of *GFAP* 3′ end alternative splicing. Hence, treatment with a

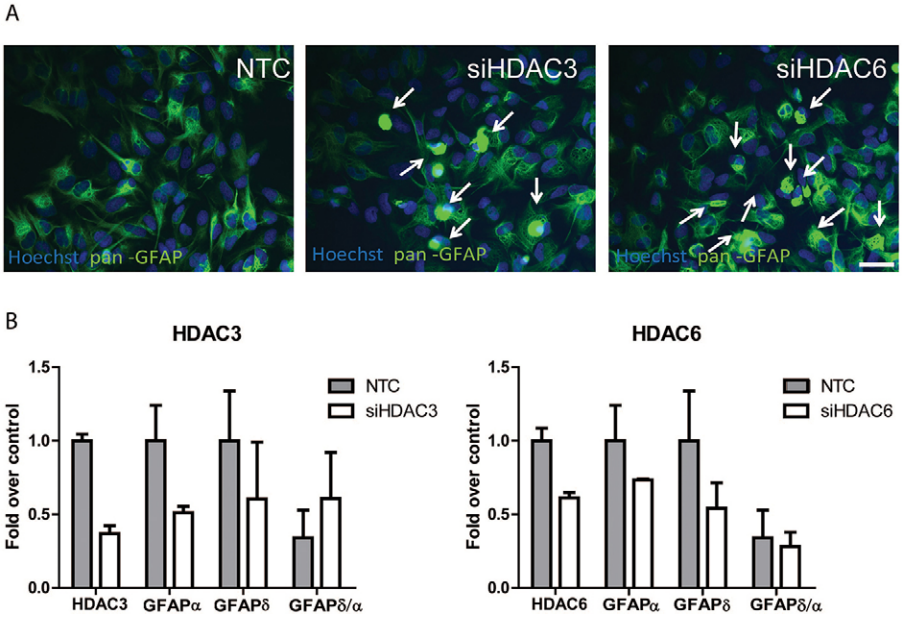

Fig. 4. Downregulation of HDAC expression using RNAi induces an aggregation of the GFAP network. The intermediate filament network of GFAP is redistributed in cells with reduced HDAC expression. (A) U343 cells were stained with a pan-GFAP antibody together with the DNA stain Hoechst 33258 at 72 hours after transfection with a control siRNA (NTC) or an siRNA targeting HDAC3 (siHDAC3) or HDAC6 (siHDAC6). Knockdown of HDAC3 or HDAC6 induced a drastic redistribution of the GFAP network, which aggregated in close proximity to the nucleus (n=2, two independent experiments). Arrows indicate cells with a reorganized intermediate filament network. Scale bar: 25 μm. (B) qPCR analysis of the *GFAPα* and *GFAPδ* transcripts upon knockdown of HDAC3 or HDAC6 for 72 hours. The *GFAPδ*:*GFAPα* ratio is also shown (n=2, two independent experiments). Data show the mean+s.e.m.

Journal of Cell Science (2014) 127, 4368–4380 doi:10.1242/jcs.145912

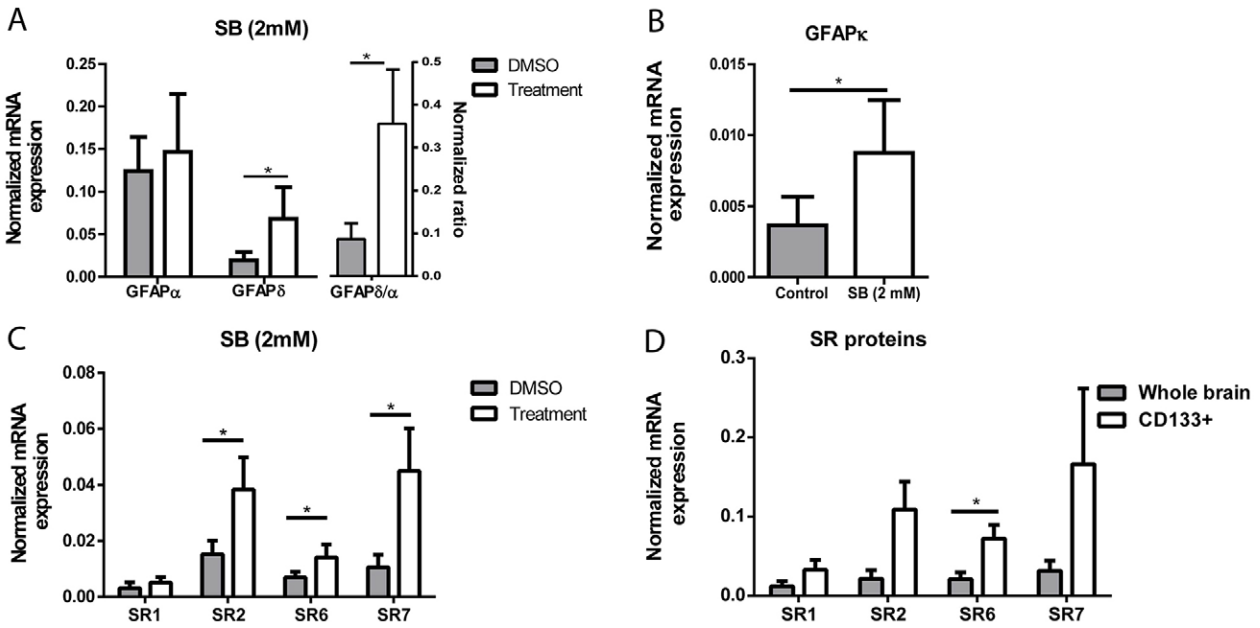

Fig. 5. A low concentration of sodium butyrate stimulates alternative splicing of *GFAP*. (A) qPCR analysis of the *GFAPα* and *GFAPδ* transcripts upon treatment of U343 cells with 2 mM sodium butyrate (SB) or vehicle for 24 hours ($n=7$). The *GFAPδ*:*GFAPα* ratio is also shown. (B,C) Expression levels of an additional alternative transcript GFAPκ (B) as well as the splicing factors SR1, SR2, SR6 and SR7 (C) are increased upon treatment with sodium butyrate ($n=7$). (D) SR proteins are highly expressed in primary human fetal NSCs. qPCR analysis of the SR proteins in fetal NSCs present in the CD133-positive fraction (CD133+) is depicted in comparison to whole brain tissue (Whole brain) ($n=5$). Data were normalized to the reference genes actin and 18S and are presented as the mean+s.e.m. *$P<0.05$.

lower concentration of sodium butyrate provides an opportunity to study the regulation of GFAP alternative splicing.

To investigate whether alternative splicing of *GFAP* is indeed induced by a low concentration of sodium butyrate, we investigated the expression levels of an additional alternatively spliced variant *GFAPκ*, which shares the 3′ end of exon 7+ but additionally contains the first 338 nucleotides of intron 7 (Blechingberg et al., 2007). Consistently, *GFAPκ* expression was also enhanced (Fig. 5B). Next, we analyzed the mRNA expression of splicing factors, which have previously been associated with the expression of the alternatively spliced transcripts of *GFAPδ* and *GFAPκ*. Expression of the mRNA encoding SR proteins 1, 2, 6 and 7 (also known as SRSF1, SRSF2, SRSF6 and SRSF7, respectively) has already been shown to increase *GFAPδ* and *GFAPκ* levels in astrocytoma cells transfected with a *GFAP* minigene. Conversely, mutating the binding sites of SR proteins reduced *GFAPδ* and *GFAPκ* levels (Blechingberg et al., 2007). In agreement with this finding, cells with increased levels of *GFAPδ* and *GFAPκ*, induced by sodium butyrate treatment, demonstrated an upregulation of the mRNAs encoding SR proteins 2, 6 and 7 and a trend towards increased expression of *SR1* (Fig. 5C). Taken together, these data show that treatment with a low concentration of sodium butyrate increased the expression of the alternatively spliced transcripts *GFAPδ* and *GFAPκ*, which was associated with an induction of splicing factors previously linked to alternative splicing of the *GFAP* 3′ end. These data suggest that an increase in histone acetylation stimulates alternative splicing of the *GFAP* gene.

Based on the observed correlation between the levels of mRNAs encoding GFAPδ and SR proteins following HDAC inhibition, we investigated whether endogenous *GFAPδ* expression is also associated with high levels of mRNAs encoding SR proteins. To this end, we analyzed primary NSCs isolated from human fetal brain, which express high levels of GFAPδ (data not shown). NSCs were isolated from brain tissue by magnetic cell sorting using CD133 (also known as prominin 1) beads as described previously (data not shown). Strikingly, in NSCs present in the CD133-positive fraction, the mRNA of SR proteins was enriched when compared to whole brain mRNA. *SR6* expression was significantly increased whereas the other SR protein mRNAs demonstrated a non-significant trend (Fig. 5D).

SR protein expression and binding regulates expression of the alternatively spliced transcript *GFAPδ*

As shown in Fig. 5, *GFAPδ* levels correlated with high expression levels of mRNAs encoding SR proteins upon HDAC inhibition in U343 cells (Fig. 5C) and in primary fetal NSCs (Fig. 5D), indicating that SR proteins might induce GFAPδ expression. To confirm that SR proteins are indeed involved in the expression of the alternatively spliced transcript *GFAPδ*, we performed a knockdown of the SR protein SR6, the mRNA levels of which strongly and significantly correlated with *GFAPδ* expression in U343 cells and in human NSCs. U343 cells were transduced with lentiviral particles encoding shRNA targeting *SR6* (shSR6) or a non-targeting shRNA (NTC). At 96 hours after transduction, expression of *SR6* was reduced by ~60% compared with its expression in NTC-treated cells (Fig. 6A, left panel). Investigation of the *GFAP* isoform expression revealed a trend towards a decrease in *GFAPδ* in the SR6-knockdown cells. *GFAPα* expression remained unchanged upon silencing of *SR6* (the ratio between control cells and SR6-knockdown cells remained close to 1), resulting in a decreased *GFAPδ*:*GFAPα* ratio (Fig. 6A, right panel). These data indicate that the presence of SR6 is necessary for GFAPδ expression. In order to investigate whether SR6 possesses a unique role in the regulation of GFAPδ expression, we

Journal of Cell Science (2014) 127, 4368–4380 doi:10.1242/jcs.145912

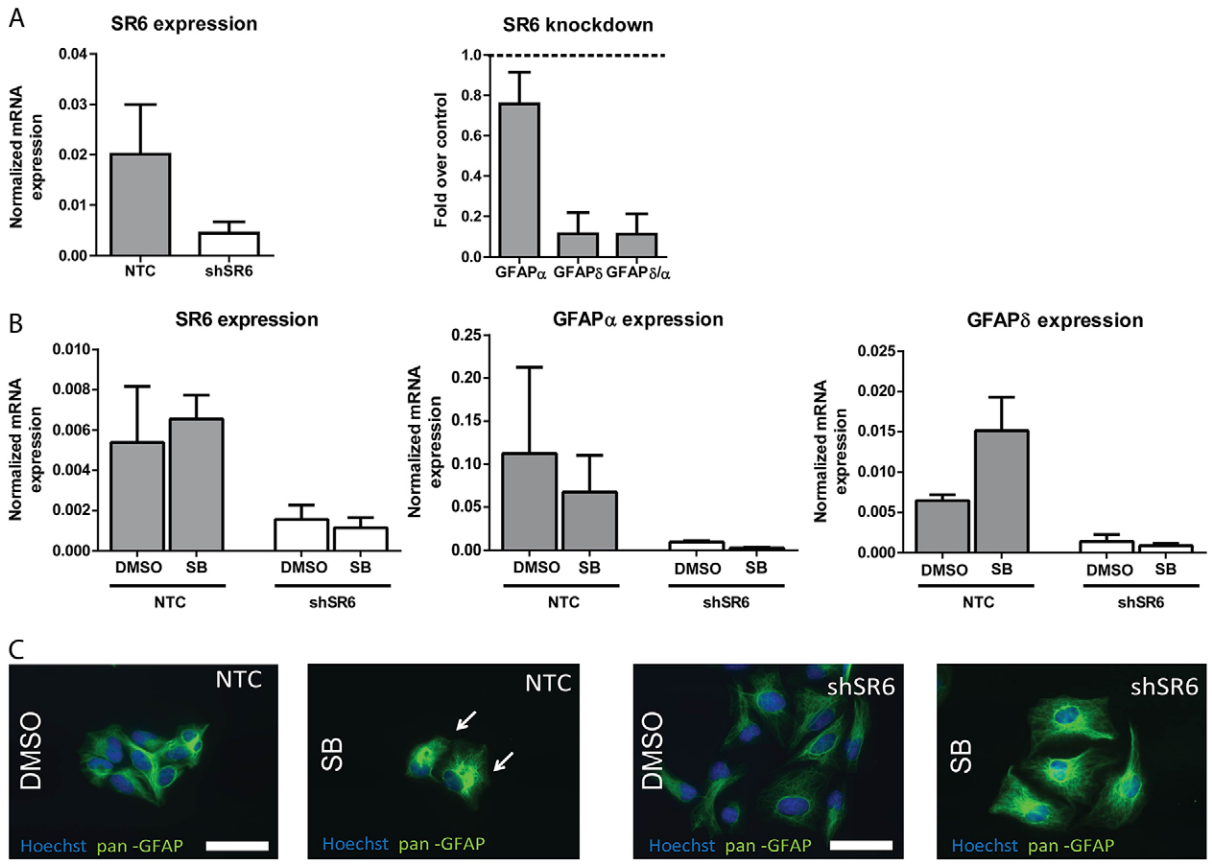

Fig. 6. Expression levels of SR proteins regulate the expression of the alternatively spliced transcript GFAPδ. (A) qPCR analysis of *SR6* (left) and the *GFAPα* and *GFAPδ* transcripts (right) upon lentiviral transduction of U343 cells with a non-targeting control shRNA (NTC) or an shRNA targeting SR6 (shSR6) for 72 hours ($n=3$). Expression of the *GFAPα* and *GFAPδ* transcripts and the *GFAPδ*:*GFAPα* ratio is depicted as fold change relative to control. (B) Expression levels of *SR6* (left) and the *GFAPα* (middle) and *GFAPδ* (right) transcripts upon treatment with vehicle (DMSO) or 2 mM sodium butyrate (SB) for 24 hours in stable lines expressing either NTC or shSR6 ($n=2$, two independent experiments). Data show the mean+s.e.m. (C) SR6 knockdown prevents aggregation of GFAP upon treatment with sodium butyrate. In cells expressing a non-targeting shRNA, a reorganization of the GFAP network was observed in U343 cells upon HDAC inhibition using 2 mM sodium butyrate. U343 cells were stained with an antibody against pan-GFAP together with the DNA stain Hoechst 33258. Sodium butyrate treatment for 72 hours induced a drastic redistribution of the GFAP network in cells expressing NTC shRNA. SR6 knockdown prevented reorganization of the GFAP network upon treatment with 2 mM sodium butyrate. Arrows indicate cells with a reorganized intermediate filament network. Scale bars: 50 μm.

performed siRNA-mediated knockdown of another SR protein, namely SR7. As shown in supplementary material Fig. S3, SR7 knockdown led to a reduction in *GFAP* expression. However, in contrast to knockdown of SR6, knockdown of SR7 induced no change in ratio between *GFAPα* and *GFAPδ*. Hence, the expression of the SR7 protein does not affect the splicing of *GFAP*. These data suggest a unique role of SR6 in the regulation of the GFAPδ:GFAPα ratio.

Moreover, we created a stable SR6-knockdown line (Fig. 6B, left panel) and treated the cells for 24 hours with 2 mM sodium butyrate. In control cells expressing a non-targeting shRNA, specifically *GFAPδ* and not *GFAPα* levels were increased upon treatment with sodium butyrate, similar to observations made in untransduced cells. Upon control treatment with DMSO, *GFAP* expression levels remained unchanged (Fig. 6B). Knockdown of SR6 was sufficient to prevent the upregulation of *GFAPδ* upon sodium butyrate treatment, which provides further evidence that the induction of the alternative transcript is dependent on SR6 expression (Fig. 6B). In line with our hypothesis, preventing *GFAPδ* induction in SR6-knockdown cells consequently prevented filament aggregation upon treatment with sodium butyrate (Fig. 6C). In cells transduced with a control shRNA, GFAP filaments aggregated in the presence of sodium butyrate. By contrast, in cells with reduced levels of SR6, no reorganization of the GFAP network was observed upon sodium butyrate treatment.

Finally, we investigated whether binding of the SR proteins to exon 7+, the alternative exon encoded in the *GFAPδ* isoform, is necessary for *GFAPδ* expression. We designed antisense oligonucleotides (AONs) complementary to the SR protein binding motifs in exon 7+. To this end, we used bioinformatic tools to predict putative SR protein binding sites (supplementary material Fig. S4A) and analyzed the secondary structure of exon 7+ to investigate the accessibility of the RNA (Fig. 7A). An AON with a low tendency for secondary structure formation was chosen to ensure efficient binding of the AON to the target region (supplementary material Fig. S4B).

Masking the binding sites with an AON interfered with exon recognition by the SR proteins. If SR proteins are crucial for the inclusion of exon 7+ and *GFAPδ* expression, blocking the binding of SR proteins is expected to result in the exclusion of exon 7+ from the transcript and a downregulation of *GFAPδ*

Journal of Cell Science (2014) 127, 4368–4380 doi:10.1242/jcs.145912

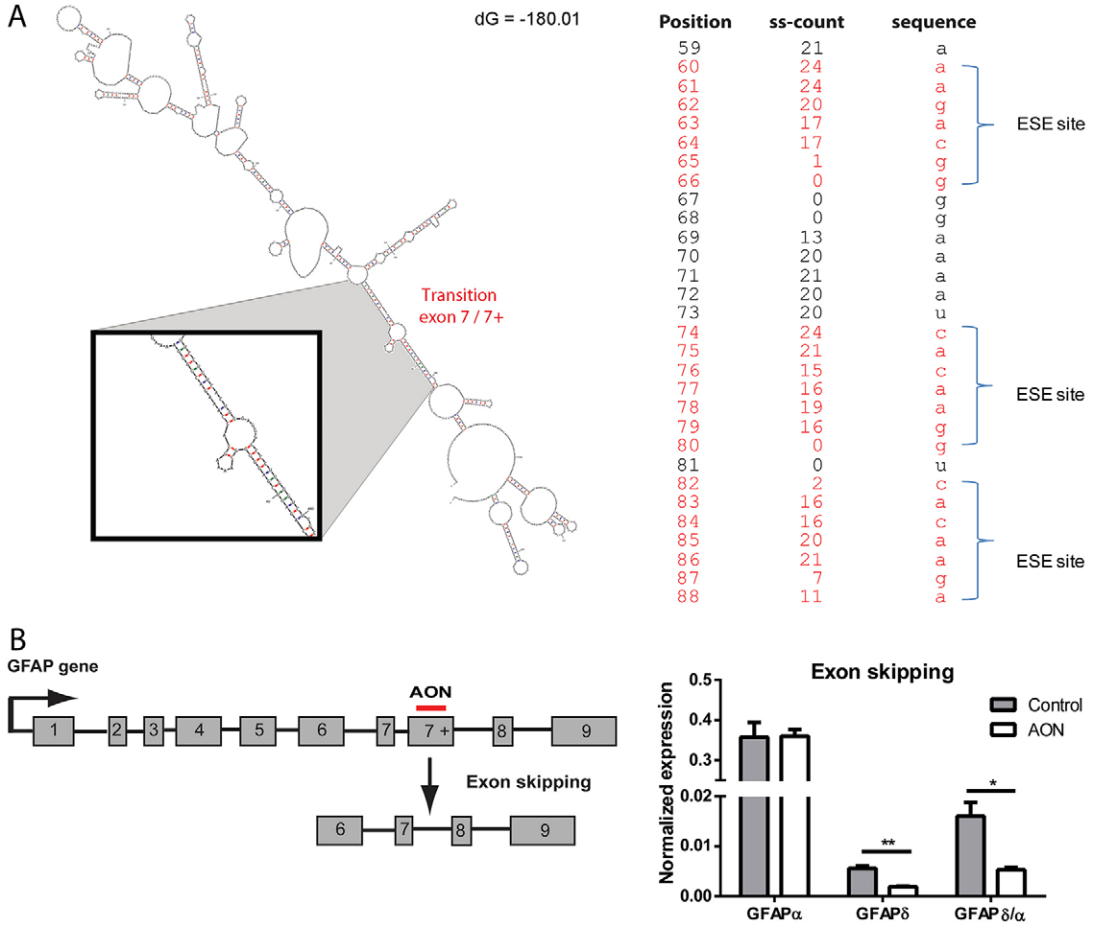

Fig. 7. Masking of the SR protein binding sites results in skipping of the alternative exon 7+ from the GFAP transcript and a downregulation of the *GFAPδ* isoform. (A) Schematic representation of the secondary structure of exons 7 and 7+ of the human GFAP gene. M-fold software was used with default settings to predict the most energetically stable secondary structure of *GFAP* mRNA. The single stranded (ss) count of transition exon 7/7+ is shown. 25 putative structures were predicted. Open structures have a high ss-count (close to 25 indicates that the nucleotide is single-stranded in the majority of structures) and closed structures have a low ss-count (e.g. a nucleotide with a score of 0 is bound to another nucleotide in all predicted structures). The selected SR binding sites show partially open structures with a high ss-count and partially closed structures with a low ss-count, which is suitable for binding of an AON. dG, ΔG (Gibbs free energy); ESE, exonic splice enhancer. (B) Left, schematic representation of the *GFAP* gene. Exons are represented by boxes and the red bar indicates the target site of the AON, which binds to SR protein binding sites. Right, human astrocytes differentiated from immortalized human NSCs were treated with synthetic AONs targeting exon 7+ or with a control AON for 72 hours. Exon skipping was assessed by q-PCR of the *GFAPα* and *GFAPδ* transcripts, and the *GFAPδ*:*GFAPα* ratio was calculated (n=3). Data were normalized to the reference genes GAPDH and 18S and are presented as the mean+s.e.m. *P<0.05, **P<0.01.

(Fig. 7B). As shown in Fig. 7B (right panel), treatment of astrocytes differentiated from a human immortalized NSC line with a synthetic AON for 72 hours indeed reduced *GFAPδ* expression significantly, whereas *GFAPα* mRNA expression remained unchanged. Silencing of the *GFAPδ* isoform when SR protein binding is blocked confirms that SR proteins are crucial for the expression of the alternatively spliced transcript *GFAPδ*.

DISCUSSION

Here, we demonstrate for the first time that histone acetylation in astrocytes is an important regulator of transcription as well as alternative splicing of *GFAP*. Inhibition of HDACs significantly reduced *GFAP* expression in primary human astrocytes as well as in astrocytoma cells. Intriguingly, upon HDAC inhibition, the ratio between the alternative transcript *GFAPδ* and the constitutive isoform *GFAPα* increased in favor of *GFAPδ* expression. A low concentration of the HDACi sodium butyrate even enhanced total amounts of *GFAPδ,* demonstrating a stimulation of alternative splicing of *GFAP*. RNAi demonstrated that expression of *GFAPδ* was dependent on the presence and binding of splicing factors of the SR protein family. At the protein level, inhibition of HDAC activity resulted in a dramatic reorganization of the GFAP network, which aggregated in close proximity to the nucleus. Importantly, not only GFAP but the whole intermediate filament network including nestin and vimentin was redistributed. Taken together, these data show that histone acetylation in astrocytes regulates (1) the transcription of *GFAP*, (2) *GFAP* isoform usage and (3) the assembly of GFAP and the whole intermediate filament network of astrocytes. A schematic overview of the effect of HDAC inhibition in astrocytes is presented in Fig. 8.

A decrease in the expression of *GFAP* might suggest that upon increased histone acetylation the astrocytes are stimulated to adapt a more immature phenotype. Mature astrocytes *in vivo* show the lowest levels of histone acetylation compared with NSCs or neurons (Hsieh et al., 2004). Furthermore, histone deacetylation is important for the differentiation of NSCs towards

Journal of Cell Science (2014) 127, 4368–4380 doi:10.1242/jcs.145912

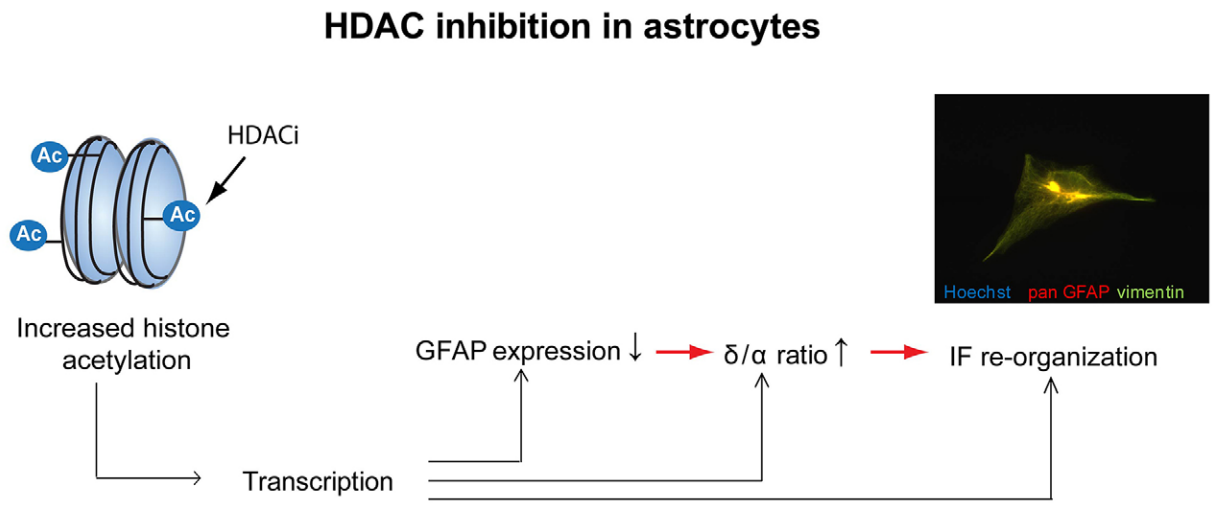

Fig. 8. Schematic overview of the effect of HDAC inhibition in astrocytes. Schematic overview of the regulation of *GFAP* transcription, isoform usage and filament assembly in astrocytes with increased histone acetylation. Inhibition of HDACs leads to increased histone acetylation (Ac) and transcriptional changes in the cell. As a result, expression of GFAP is decreased, whereas the *GFAPδ*:*GFAPα* ratio is increased. Moreover, the intermediate filament (IF) proteins GFAP and vimentin are redistributed in the presence of increased histone acetylation. According to our hypothesis, and as depicted by red arrows, reduced transcription of *GFAP* favors expression of the alternative transcript *GFAPδ*, which leads to an increase in the *GFAPδ*:*GFAPα* ratio and aggregation of the intermediate filament network. Hence, changes in the *GFAP* expression levels and a different isoform usage might lead to a reorganization of the intermediate filament network, which aggregates next to the nucleus.

astrocytes, which are marked by GFAP expression (Asano et al., 2009). By increasing the amount of histone acetylation in astrocytes with HDACi, the maturation state of the astrocytes might be affected. This hypothesis is further supported by the change in the *GFAP* isoform ratio in favor of *GFAPδ* expression. In mature human astrocytes, expression of the alternative transcript *GFAPδ* is low, whereas *GFAPα* represents the predominant *GFAP* transcript, indicating low alternative splicing of *GFAP* (Roelofs et al., 2005). As our data demonstrate, HDAC inhibition enhances *GFAPδ* expression relative to that of the canonical form *GFAPα*. Conversely, low acetylation levels in differentiated astrocytes might reduce alternative splicing of *GFAP*, resulting in low *GFAPδ* but high *GFAPα* expression. The specific function and the role of GFAPδ is still unknown. Its high expression in NSCs suggests that GFAPδ might play a specific role in the formation of the intermediate filament network in NSCs and is not of importance after differentiation into astrocytes.

The observed change in *GFAP* isoform usage depending on the transcription rate of the gene is in line with a close interaction between transcription and alternative splicing. Our data suggest that upon decreased H3K27 acetylation at the GFAP promoter (Fig. 2), the chromatin might be more condensed, reducing the transcriptional speed and increasing GFAPδ splicing. There are two possible hypotheses that might explain a causal relationship between epigenetic modifications and alternative splicing. The first hypothesis states that a decrease in histone acetylation could reduce the RNA Pol II elongation rate; thus, co-transcriptional splicing is altered upon a changed transcriptional velocity. The second hypothesis states that histone acetylation marks can be recognized by adaptor proteins that, in turn, recruit splicing factors to the pre-mRNA and thereby regulate alternative splicing (Luco et al., 2011). Both mechanisms could take place at the *GFAP* gene depending on the degree of acetylation.

In line with the first hypothesis, the ratio between constitutive and alternatively spliced isoforms increased in association with lower *GFAP* transcription levels induced by HDAC inhibition, suggesting a dependency on transcriptional speed. A correlation of promoter activity and alternative splicing of *GFAP* has been previously demonstrated for a *GFAP* minigene. Total *GFAP* expression is enhanced upon increased promoter activity of the minigene, but the increase in the expression of the alternative forms δ and κ was less pronounced (Blechingberg et al., 2007). An effect of transcriptional speed on alternative splicing of the endogenous *GFAP* gene in astrocytes was confirmed here. Decreased transcription of *GFAP* upon HDAC inhibition resulted in a more pronounced reduction in the expression of *GFAPα* than that of *GFAPδ*. This indicates that at lower *GFAP* promoter activity, alternative splice site usage decreases less than constitutive splice site usage, thus resulting in an increase in the *GFAPδ*:*GFAPα* ratio.

At low concentrations of sodium butyrate, alternative splicing of *GFAP* was induced in a manner that was dependent on the expression and binding of SR proteins. Upregulation of SR protein expression upon stimulation of *GFAPδ* expression suggests the involvement of a chromatin adaptor model in the regulation of *GFAPδ* expression. Recognition of the acetylation marks in exon 7+ by an adaptor protein could be responsible for the recruitment of the SR splicing factors to exon 7+, thereby inducing its inclusion in the transcript (Luco et al., 2011). Enrichment of the expression of mRNAs encoding SR proteins in primary human NSCs with high endogenous levels of *GFAPδ* further supports this hypothesis. An experiment that combines HDAC inhibition and stable expression of an AON that blocks SR protein binding sites (Fig. 7) could determine whether SR protein binding is crucial for the upregulation of *GFAPδ* upon HDAC inhibition.

Dysregulation of SR protein binding has been previously associated with human disease. Cartegni and colleagues have demonstrated that 50% of mutations in human genes that are associated with exon skipping disrupt one or more binding motifs of SR proteins (Cartegni et al., 2002). In addition, dysregulation of SR protein expression has been linked to cancer. Expression

Journal of Cell Science (2014) 127, 4368–4380 doi:10.1242/jcs.145912

levels of SR6, identified here as a crucial regulator of *GFAP* alternative splicing, have been found to be elevated in breast tumor tissue, in association with changes in CD44 alternative splicing (Huang et al., 2007). *In vitro* data suggest a role for CD44 alternative splicing in epithelial–mesenchymal transition and cancer progression (Brown et al., 2011). Based on these findings, future studies are necessary to investigate a possible regulatory role of SR6 in CD44 splicing and, consequently, the formation and progression of breast cancer.

Recently, dysregulation of alternative splicing of *GFAP* was associated with leukodystrophies, rare genetic disorders that affect glial cells in the white matter of the central nervous system. Astrocytes of patients with vanishing white matter (VWM) disease, a genetic disorder involving mutations in the eukaryotic translation initiation factor 2B (eIF2B), show a specific overexpression of GFAPδ but not GFAPα, resulting in an increase in the GFAPδ:GFAPα ratio (Huyghe et al., 2012; Bugiani et al., 2011). Correlating with high GFAPδ expression, a reduction in the mRNA levels of hnRNPH1, hnRNPF and hnRNPC was observed (Huyghe et al., 2012). Intriguingly, proteins of the hnRNP family influence the inclusion of exons by binding to SR protein binding sites to inhibit SR protein binding (Wahl et al., 2009). The crucial importance of SR protein binding for *GFAPδ* expression shown in this study strongly suggests that reduced hnRNP levels and subsequently increased SR protein binding to exon 7+ is responsible for the induction of GFAPδ expression in patients with VWM disease. This example highlights the importance of a tight regulation of the splicing process with direct implications for human diseases.

Interestingly, in VWM disease as well as AxD, a genetic disorder characterized by heterozygous mutations in *GFAP* itself (Quinlan et al., 2007), dysregulation of GFAP expression is associated with abnormal astrocyte morphology. In patients with VWM disease, astrocytes display short processes in comparison to the fine arborisations of astrocytes in control tissue (Huyghe et al., 2012). In AxD, mutations in *GFAP* result in the aggregation of the mutant protein in 'Rosenthal fibers', a hallmark of the disease (Quinlan et al., 2007; Flint et al., 2012). As previously discussed, aggregation of the GFAP network and changes in the astrocyte morphology might contribute to similarities in the clinical phenotype of patients carrying mutations in *eIF2B* or *GFAP* (Huyghe et al., 2012).

Here, we demonstrate that suppression of histone acetylation triggers a reorganization of the GFAP network. This is the first report on aggregation of the endogenous GFAP protein and additional intermediate filament proteins vimentin and nestin *in vitro*. Previously, general GFAP overexpression or incorporation of high concentrations of GFAPδ in an existing GFAP network has been shown to result in compromised assembly of the GFAP filaments (Kamphuis et al., 2012; Roelofs et al., 2005; Nielsen et al., 2002). The data presented here indicate that an increased *GFAPδ*:*GFAPα* ratio in the presence of reduced *GFAP* transcription can also lead to reorganization of the GFAP network and the whole intermediate filament network. As our data show, histone acetylation is a crucial regulator of this process.

A link between histone acetylation and altered GFAP expression and aggregation was recently reported in the context of AxD. Interestingly, an AxD patient was identified who carried, in addition to a mutation in the *GFAP* gene, a mutation in the *HDAC6* gene, which was associated with a more severe phenotype of AxD (Melchionda et al., 2013). The mutated HDAC6 protein displayed reduced histone deacetylation activity, partially resembling the general HDAC inhibition performed in our study. Moreover, *HDAC6* mutation in fibroblasts caused an aggregation of acetylated α-tubulin in the perinuclear region, indicating dysregulation of the microtubule-organizing centre. Because the intermediate filament network and microtubules are closely interconnected to form the cytoskeleton of a cell, an aggregation of acetylated α-tubulin might influence intermediate filament organization. Consistently, an HDAC6-dependent collapse of the intermediate filament vimentin was recently described. The authors suggest that, dependent on HDAC6 activity, changes in the acetylation of microtubules lead to a reorganization of the vimentin network (Rathje et al., 2014). By analogy, mutations in *HDAC6* and *GFAPδ* in AxD patients might synergistically trigger a reorganization of the GFAP network and an abnormal morphology of astrocytes.

We observed upon HDAC inhibition that histone acetylation at the GFAP promoter is reduced (Fig. 2) and that no changes in histone acetylation on other GFAP regulatory elements occur (data not shown). These data suggest that HDAC inhibition might not directly act on the *GFAP* gene. Moreover, HDAC activity might have a direct effect on the acetylation of the GFAP protein. Acetylation of GFAP has been reported in the context of amyotrophic lateral sclerosis (Liu et al., 2013). Whether acetylation of the GFAP protein is involved in the regulation of GFAP filament assembly is still unclear.

Together with our finding of a reorganization of the intermediate filament network upon HDAC inhibition, the data from AxD suggests that HDACs could have a modulatory role in diseases involving abnormal morphology of astrocytes associated with GFAP dysregulation. Aggregation of the GFAP network was associated with incomplete maturation of astrocytes in patients with leukodystrophy (Mignot et al., 2004). In line with a role of HDACs in this process, our data show that HDAC inhibition might influence the maturation of astrocytes by reducing total *GFAP* expression and decreasing the *GFAPδ*:*GFAPα* ratio, which resembles a more immature pattern of *GFAP* expression.

In conclusion, our data from primary human astrocytes and astrocytoma cells demonstrate that inhibition of HDACs results in reduced transcription of *GFAP* and, in agreement with our hypothesis, a differential isoform usage. Decreased transcription of *GFAP* favored expression of the alternative *GFAPδ* isoform dependent on the binding of splice regulators of the SR proteins family. Moreover, a disturbance of the tight regulation of histone acetylation in astrocytes induced aggregation not only of GFAP filaments but of the whole intermediate filament network in astrocytes. Taken together, these data show that histone acetylation in astrocytes regulates (1) transcription of *GFAP*, (2) *GFAP* isoform usage and (3) the assembly of GFAP and the whole intermediate filament network of astrocytes.

MATERIALS AND METHODS

Cell culture

All cells were cultured at 37℃ under a humidified 5% CO_2, 95% air atmosphere. U343 astrocytoma cells were cultured in a 1:1 mixture of high-glucose Dulbecco's modified Eagle medium (DMEM, Gibco, Invitrogen, Carlsbad, CA) and F10 HAM (Gibco, Invitrogen) supplemented with 10% fetal bovine serum (FBS) and 1% penicillin-streptomycin (all Invitrogen).

Isolation of primary human astrocytes and fetal NSCs

Isolation of primary human astrocytes was performed as described previously (Smolders et al., 2013). Fetal brain tissue (gestational week 14–17, $n=5$) was obtained from spontaneous or medically induced abortions with appropriate maternal written consent for abortion. Tissue

was obtained in accordance with the Declaration of Helsinki and the Academic Medical Centre (AMC) Research Code provided by the Medical Ethics Committee of the AMC, Amsterdam, The Netherlands. All autopsies were performed within 12 hours after abortion.

For isolation of NSCs, fetal brain tissue was collected in 10 ml of cold Hibernate (Invitrogen), mechanically dissociated into small pieces, and digested with 0.2% trypsin and 0.1% DNase I (Invitrogen) for 5 minutes at 37℃ with shaking. Next, 1 ml of FBS was added to the mixture and subsequently the cells were collected by centrifugation. The pellet was taken up in DMEM without Phenol Red containing 10% FBS, 2.5% HEPES and 1% penicillin-streptomycin (all Invitrogen). Percoll (Amersham/GE Healthcare) was added (half of cell suspension volume), and this mixture was centrifuged at 3220 ***g***, 4℃ for 20 minutes. The second layer (glial-cell-containing fraction) was collected and washed with DMEM+GlutaMAX containing 10% FBS, 1% penicillin-streptomycin, 2.5% HEPES and 1% gentamycin (all Invitrogen). After centrifugation (239 ***g***, 10 minutes), the cell pellet was taken up in beads buffer [phosphate-buffered saline (PBS), pH 7.2, 0.5% bovine serum albumin (BSA) and 2 mM EDTA]. Then, $CD133^{+}$ cells were isolated using a magnetic separation system (MACS; Miltenyi Biotec) following the manufacturer's description. After isolation, cells were collected by centrifugation (153 ***g***, 5 minutes) and the pellet was stored at −20℃.

Cell treatments

The HDAC inhibitors trichostatin A (TSA) and sodium butyrate were obtained from Sigma-Aldrich (St Louis, MO). Cells were treated for 24, 48 or 72 hours with a final concentration of 330 nM or 660 nM TSA. Ethanol (final concentration of 0.3%) was applied in the control condition, as TSA was dissolved in ethanol. Alternatively, cells were treated with 2 mM or 5 mM sodium butyrate or DMSO (0.01%).

To block the binding of SR proteins, cells were treated for 72 hours with a synthetic antisense oligonucleotide (AON) with the following sequence; 5′-CUUGUGAUUUUCCCCGUCUUUGG-3′. The AON is directed against SR protein binding motifs encoded in exon 7+ of the human *GFAP* gene. The AON consists of 2′-O-methyl-modified ribose molecules and a full-length phosphorothioate backbone (Eurogentec, Belgium). As control, a non-targeting AON was added with the sequence 5′-GCAAGAUGCCAGCAGA-3′ (encoding the sense sequence targeting exon 19 of the dystrophin gene; a kind gift from Annemieke Aartsma-Rus). The culture medium was supplemented with oligonucleotides at a concentration of 200 nM and was replaced every day during the experiment. Treatment conditions were optimized with a control AON carrying a 5′-fluorescein label to visualize the uptake of the antisense nucleotides (data not shown). Exon skipping was performed in human astrocytes, which were differentiated from an immortalized fetal neural stem cell line (De Filippis et al., 2007). The low proliferation rate compared with that of astrocytoma cells prevented a 'wash-out' of the AON due to frequent cell divisions.

siRNA transfections and lentiviral transduction

For the HDAC6 and HDAC3 knockdown studies, U343 cells were plated in 24-well plates, at a density of 50,000 cells per well in 500 µl of culture medium. The next day, medium was replaced with 500 µl of fresh culture medium without antibiotics. Then, cells were transfected using 3 µl of a 20 µM siRNA stock [siGENOME HDAC6 siRNA (M-003499-00-0005), ON-TARGETplus human HDAC3 siRNA (L-003496-00-0005) or non-targeting siRNA (D-001210-02-05), all from Thermo Scientific], together with 1 µl of Lipofectamine 2000 (Invitrogen) per well, following the manufacturer's instructions. After 72 hours, cells were collected in Trizol for mRNA analysis or fixed with 4% formalin for 10 minutes at room temperature for immunofluorescent staining. Lentiviral production and *in vitro* transduction were performed as described previously (Moeton et al., 2014).

Chromatin immunoprecipitation

Chromatin immunoprecipitation was performed as described previously (Creyghton et al., 2010).

RNA isolation, cDNA synthesis and quantitative real-time PCR

For RNA isolation, cells were harvested and total RNA was isolated with Trizol (Invitrogen) according to the manufacturer's protocol. The resulting RNA pellet was dissolved in RNase free water. The RNA concentration was determined using a NanoDrop ND-1000 spectrophotometer 7 (NanoDrop Technologies, Wilmington, DE). The reverse transcriptase and qPCR reactions were performed as described previously (Kamphuis et al., 2012). The primers used in this study are listed in supplementary material Table S1.

Western blot analysis and immunocytochemistry

Western blot analysis was performed as described previously (Moeton et al., 2014). The antibodies used are listed in supplementary material Table S2.

Statistical analysis

Data were analyzed using GraphPad Prism software (GraphPad Software, San Diego, CA). All data are presented as the mean+s.e.m. To eliminate intra-experimental variation, we applied a factor correction tool as described previously (Ruijter et al., 2006). A Kolgmorov–Smirnov test was performed to test for a normal distribution. If a normal distribution was confirmed, a Student's *t*-test was performed. Alternatively, a non-parametric Mann–Whitney test was applied. Differences amongst groups were considered to be significant at $P<0.05$.

Acknowledgements

The authors would like to thank Martina Moeton (Astrocyte Biology & Neurodegeneration, Netherlands Institute for Neuroscience, Amsterdam, The Netherlands) for her advice and stimulating discussions. Moreover, the authors are grateful to Sasja Heetveld and Peter Heutink (both at Deutsches Zentrum für Neurodegenerative Erkrankungen,Tübingen Germany) for providing the shRNA vectors and to Annemieke Aartsma-Rus (Center for Human and Clinical Genetics, Leiden University Medical Center, Leiden, The Netherlands) for her advice on the design of the AONs and for providing the control AON for exon skipping. The authors would like to thank Kees Weijer (Department of Cell Biology and Histology, AMC, Amsterdam, The Netherlands) for the collection of brain tissue.

Competing interests

The authors declare no competing interests.

Author contributions

R.K., P.v.T., M.E.v.S. and E.M.H conceived of and designed the study; data were collected by R.K., M.A.M.S., E.J.v.B., J.A.S., W.K., M.W.V. and M.E.v.S., and were assembled by R.K., M.A.M.S., E.J.v.B., J.A.S., W.K. and M.P.C.; data were analyzed and interpreted by R.K. and M.A.M.S; and the manuscript was written by R.K., P.v.T. and E.M.H. L.D. and A.V. provided human neural stem cell lines and information on their use; E.A. provided fetal human brain tissue for neural stem cell isolation; and M.P.C. provided expertise on chromatin analysis. E.M.H. secured funding for the project and approved the final manuscript.

Funding

This project was funded by the Netherlands Organization for Scientific Research (NWO) VICI grant to E.M.H. [grant number 865.09.003]; and the European Union FP7 project DEVELAGE [grant number N 278486] EA; and *NanoNet* COST Action [grant number BM1002].

Supplementary material

Supplementary material available online at
http://jcs.biologists.org/lookup/suppl/doi:10.1242/jcs.145912/-/DC1

References

Ajamian, F., Salminen, A. and Reeben, M. (2004). Selective regulation of class I and class II histone deacetylases expression by inhibitors of histone deacetylases in cultured mouse neural cells. *Neurosci. Lett.* **365**, 64-68.

Alexander, W. S. (1949). Progressive fibrinoid degeneration of fibrillary astrocytes associated with mental retardation in a hydrocephalic infant. *Brain* **72**, 373-381.

Andreiuolo, F., Junier, M. P., Hol, E. M., Miquel, C., Chimelli, L., Leonard, N., Chneiweiss, H., Daumas-Duport, C. and Varlet, P. (2009). GFAPdelta immunostaining improves visualization of normal and pathologic astrocytic heterogeneity. *Neuropathology* **29**, 31-39.

Asano, H., Aonuma, M., Sanosaka, T., Kohyama, J., Namihira, M. and Nakashima, K. (2009). Astrocyte differentiation of neural precursor cells is enhanced by retinoic acid through a change in epigenetic modification. *Stem Cells* **27**, 2744-2752.

Blechingberg, J., Lykke-Andersen, S., Jensen, T. H., Jørgensen, A. L. and Nielsen, A. L. (2007). Regulatory mechanisms for 3′-end alternative splicing and polyadenylation of the Glial Fibrillary Acidic Protein, GFAP, transcript. *Nucleic Acids Res.* **35**, 7636-7650.

Boyd, S. E., Nair, B., Ng, S. W., Keith, J. M. and Orian, J. M. (2012). Computational characterization of 3′ splice variants in the GFAP isoform family. *PLoS ONE* **7**, e33565.

Brown, R. L., Reinke, L. M., Damerow, M. S., Perez, D., Chodosh, L. A., Yang, J. and Cheng, C. (2011). CD44 splice isoform switching in human and mouse epithelium is essential for epithelial-mesenchymal transition and breast cancer progression. *J. Clin. Invest.* **121**, 1064-1074.

Bugiani, M., Boor, I., van Kollenburg, B., Postma, N., Polder, E., van Berkel, C., van Kesteren, R. E., Windrem, M. S., Hol, E. M., Scheper, G. C. et al. (2011). Defective glial maturation in vanishing white matter disease. *J. Neuropathol. Exp. Neurol.* **70**, 69-82.

Cartegni, L., Chew, S. L. and Krainer, A. R. (2002). Listening to silence and understanding nonsense: exonic mutations that affect splicing. *Nat. Rev. Genet.* **3**, 285-298.

Cheng, P.-Y., Lin, Y.-P., Chen, Y.-L., Lee, Y.-C., Tai, C.-C., Wang, Y.-T., Chen, Y.-J., Kao, C.-F. and Yu, J. (2011). Interplay between SIN3A and STAT3 mediates chromatin conformational changes and GFAP expression during cellular differentiation. *PLoS ONE* **6**, e22018.

Choi, K. C., Kwak, S. E., Kim, J. E., Sheen, S. H. and Kang, T. C. (2009). Enhanced glial fibrillary acidic protein-delta expression in human astrocytic tumor. *Neurosci. Lett.* **463**, 182-187.

Creyghton, M. P., Cheng, A. W., Welstead, G. G., Kooistra, T., Carey, B. W., Steine, E. J., Hanna, J., Lodato, M. A., Frampton, G. M., Sharp, P. A. et al. (2010). Histone H3K27ac separates active from poised enhancers and predicts developmental state. *Proc. Natl. Acad. Sci. USA* **107**, 21931-21936.

Dangond, F. and Gullans, S. R. (1998). Differential expression of human histone deacetylase mRNAs in response to immune cell apoptosis induction by trichostatin A and butyrate. *Biochem. Biophys. Res. Commun.* **247**, 833-837.

De Filippis, L., Lamorte, G., Snyder, E. Y., Malgaroli, A. and Vescovi, A. L. (2007). A novel, immortal, and multipotent human neural stem cell line generating functional neurons and oligodendrocytes. *Stem Cells* **25**, 2312-2321.

de Pablo, Y., Nilsson, M., Pekna, M. and Pekny, M. (2013). Intermediate filaments are important for astrocyte response to oxidative stress induced by oxygen-glucose deprivation and reperfusion. *Histochem. Cell Biol.* **140**, 81-91.

Duan, H., Heckman, C. A. and Boxer, L. M. (2005). Histone deacetylase inhibitors down-regulate bcl-2 expression and induce apoptosis in t(14;18) lymphomas. *Mol. Cell. Biol.* **25**, 1608-1619.

Fan, G., Martinowich, K., Chin, M. H., He, F., Fouse, S. D., Hutnick, L., Hattori, D., Ge, W., Shen, Y., Wu, H. et al. (2005). DNA methylation controls the timing of astrogliogenesis through regulation of JAK-STAT signaling. *Development* **132**, 3345-3356.

Flint, D., Li, R., Webster, L. S., Naidu, S., Kolodny, E., Percy, A., van der Knaap, M., Powers, J. M., Mantovani, J. F., Ekstein, J. et al. (2012). Splice site, frameshift, and chimeric GFAP mutations in Alexander disease. *Hum. Mutat.* **33**, 1141-1148.

Gibbons, H. M., Hughes, S. M., Van Roon-Mom, W., Greenwood, J. M., Narayan, P. J., Teoh, H. H., Bergin, P. M., Mee, E. W., Wood, P. C., Faull, R. L. et al. (2007). Cellular composition of human glial cultures from adult biopsy brain tissue. *J. Neurosci. Methods* **166**, 89-98.

Hagemann, T. L., Gaeta, S. A., Smith, M. A., Johnson, D. A., Johnson, J. A. and Messing, A. (2005). Gene expression analysis in mice with elevated glial fibrillary acidic protein and Rosenthal fibers reveals a stress response followed by glial activation and neuronal dysfunction. *Hum. Mol. Genet.* **14**, 2443-2458.

Hnilicová, J., Hozeifi, S., Dušková, E., Icha, J., Tománková, T. and Staněk, D. (2011). Histone deacetylase activity modulates alternative splicing. *PLoS ONE* **6**, e16727.

Hsieh, J., Nakashima, K., Kuwabara, T., Mejia, E. and Gage, F. H. (2004). Histone deacetylase inhibition-mediated neuronal differentiation of multipotent adult neural progenitor cells. *Proc. Natl. Acad. Sci. USA* **101**, 16659-16664.

Huang, C. S., Shen, C. Y., Wang, H. W., Wu, P. E. and Cheng, C. W. (2007). Increased expression of SRp40 affecting CD44 splicing is associated with the clinical outcome of lymph node metastasis in human breast cancer. *Clin. Chim. Acta* **384**, 69-74.

Huyghe, A., Horzinski, L., Hénaut, A., Gaillard, M., Bertini, E., Schiffmann, R., Rodriguez, D., Dantal, Y., Boespflug-Tanguy, O. and Fogli, A. (2012). Developmental splicing deregulation in leukodystrophies related to EIF2B mutations. *PLoS ONE* **7**, e38264.

Jing, R., Wilhelmsson, U., Goodwill, W., Li, L., Pan, Y., Pekny, M. and Skalli, O. (2007). Synemin is expressed in reactive astrocytes in neurotrauma and interacts differentially with vimentin and GFAP intermediate filament networks. *J. Cell Sci.* **120**, 1267-1277.

Kamphuis, W., Mamber, C., Moeton, M., Kooijman, L., Sluijs, J. A., Jansen, A. H., Verveer, M., de Groot, L. R., Smith, V. D., Rangarajan, S. et al. (2012). GFAP isoforms in adult mouse brain with a focus on neurogenic astrocytes and reactive astrogliosis in mouse models of Alzheimer disease. *PLoS ONE* **7**, e42823.

Kanski, R., van Strien, M. E., van Tijn, P. and Hol, E. M. (2014). A star is born: new insights into the mechanism of astrogenesis. *Cell. Mol. Life Sci.* **71**, 433-447.

Kornblihtt, A. R., de la Mata, M., Fededa, J. P., Munoz, M. J. and Nogues, G. (2004). Multiple links between transcription and splicing. *RNA* **10**, 1489-1498.

Liu, D., Liu, C., Li, J., Azadzoi, K., Yang, Y., Fei, Z., Dou, K., Kowall, N. W., Choi, H. P., Vieira, F. et al. (2013). Proteomic analysis reveals differentially regulated protein acetylation in human amyotrophic lateral sclerosis spinal cord. *PLoS ONE* **8**, e80779.

Long, J. C. and Caceres, J. F. (2009). The SR protein family of splicing factors: master regulators of gene expression. *Biochem. J.* **417**, 15-27.

Luco, R. F., Pan, Q., Tominaga, K., Blencowe, B. J., Pereira-Smith, O. M. and Misteli, T. (2010). Regulation of alternative splicing by histone modifications. *Science* **327**, 996-1000.

Luco, R. F., Allo, M., Schor, I. E., Kornblihtt, A. R. and Misteli, T. (2011). Epigenetics in alternative pre-mRNA splicing. *Cell* **144**, 16-26.

Martinian, L., Boer, K., Middeldorp, J., Hol, E. M., Sisodiya, S. M., Squier, W., Aronica, E. and Thom, M. (2009). Expression patterns of glial fibrillary acidic protein (GFAP)-delta in epilepsy-associated lesional pathologies. *Neuropathol. Appl. Neurobiol.* **35**, 394-405.

Melchionda, L., Fang, M., Wang, H., Fugnanesi, V., Morbin, M., Liu, X., Li, W., Ceccherini, I., Farina, L., Savoiardo, M. et al. (2013). Adult-onset alexander disease, associated with a mutation in an alternative GFAP transcript, may be phenotypically modulated by a non-neutral HDAC6 variant. *Orphanet J. Rare Dis.* **8**, 66.

Messing, A., Head, M. W., Galles, K., Galbreath, E. J., Goldman, J. E. and Brenner, M. (1998). Fatal encephalopathy with astrocyte inclusions in GFAP transgenic mice. *Am. J. Pathol.* **152**, 391-398.

Middeldorp, J. and Hol, E. M. (2011). GFAP in health and disease. *Prog. Neurobiol.* **93**, 421-443.

Mignot, C., Boespflug-Tanguy, O., Gelot, A., Dautigny, A., Pham-Dinh, D. and Rodriguez, D. (2004). Alexander disease: putative mechanisms of an astrocytic encephalopathy. *Cell. Mol. Life Sci.* **61**, 369-385.

Moeton, M., Kanski, R., Stassen, O. M., Sluijs, J. A., Geerts, D., van Tijn, P., Wiche, G., van Strien, M. E. and Hol, E. M. (2014). Silencing GFAP isoforms in astrocytoma cells disturbs laminin-dependent motility and cell adhesion. *FASEB J.* **28**, 2942-2954.

Namihira, M., Kohyama, J., Semi, K., Sanosaka, T., Deneen, B., Taga, T. and Nakashima, K. (2009). Committed neuronal precursors confer astrocytic potential on residual neural precursor cells. *Dev. Cell* **16**, 245-255.

Nawashiro, H., Messing, A., Azzam, N. and Brenner, M. (1998). Mice lacking GFAP are hypersensitive to traumatic cerebrospinal injury. *Neuroreport* **9**, 1691-1696.

Nawashiro, H., Brenner, M., Fukui, S., Shima, K. and Hallenbeck, J. M. (2000). High susceptibility to cerebral ischemia in GFAP-null mice. *J. Cereb. Blood Flow Metab.* **20**, 1040-1044.

Nielsen, A. L., Holm, I. E., Johansen, M., Bonven, B., Jørgensen, P. and Jørgensen, A. L. (2002). A new splice variant of glial fibrillary acidic protein, GFAP epsilon, interacts with the presenilin proteins. *J. Biol. Chem.* **277**, 29983-29991.

Otani, N., Nawashiro, H., Fukui, S., Ooigawa, H., Ohsumi, A., Toyooka, T., Shima, K., Gomi, H. and Brenner, M. (2006). Enhanced hippocampal neurodegeneration after traumatic or kainate excitotoxicity in GFAP-null mice. *J. Clin. Neurosci.* **13**, 934-938.

Perng, M. D., Wen, S. F., Gibbon, T., Middeldorp, J., Sluijs, J., Hol, E. M. and Quinlan, R. A. (2008). Glial fibrillary acidic protein filaments can tolerate the incorporation of assembly-compromised GFAP-delta, but with consequences for filament organization and alphaB-crystallin association. *Mol. Biol. Cell* **19**, 4521-4533.

Puppin, C., Passon, N., Franzoni, A., Russo, D. and Damante, G. (2011). Histone deacetylase inhibitors control the transcription and alternative splicing of prohibitin in thyroid tumor cells. *Oncol. Rep.* **25**, 393-397.

Quinlan, R. A., Brenner, M., Goldman, J. E. and Messing, A. (2007). GFAP and its role in Alexander disease. *Exp. Cell Res.* **313**, 2077-2087.

Rada-Iglesias, A., Enroth, S., Ameur, A., Koch, C. M., Clelland, G. K., Respuela-Alonso, P., Wilcox, S., Dovey, O. M., Ellis, P. D., Langford, C. F. et al. (2007). Butyrate mediates decrease of histone acetylation centered on transcription start sites and down-regulation of associated genes. *Genome Res.* **17**, 708-719.

Rathje, L. S., Nordgren, N., Pettersson, T., Rönnlund, D., Widengren, J., Aspenström, P. and Gad, A. K. (2014). Oncogenes induce a vimentin filament collapse mediated by HDAC6 that is linked to cell stiffness. *Proc. Natl. Acad. Sci. USA* **111**, 1515-1520.

Reid, G., Métivier, R., Lin, C. Y., Denger, S., Ibberson, D., Ivacevic, T., Brand, H., Benes, V., Liu, E. T. and Gannon, F. (2005). Multiple mechanisms induce transcriptional silencing of a subset of genes, including oestrogen receptor alpha, in response to deacetylase inhibition by valproic acid and trichostatin A. *Oncogene* **24**, 4894-4907.

Roelofs, R. F., Fischer, D. F., Houtman, S. H., Sluijs, J. A., Van Haren, W., Van Leeuwen, F. W. and Hol, E. M. (2005a). Adult human subventricular, subgranular, and subpial zones contain astrocytes with a specialized intermediate filament cytoskeleton. *Glia* **52**, 289-300.

Ruijter, J. M., Thygesen, H. H., Schoneveld, O. J., Das, A. T., Berkhout, B. and Lamers, W. H. (2006). Factor correction as a tool to eliminate between-session variation in replicate experiments: application to molecular biology and retrovirology. *Retrovirology* **3**, 2.

Smolders, J., Schuurman, K. G., van Strien, M. E., Melief, J., Hendrickx, D., Hol, E. M., van Eden, C., Luchetti, S. and Huitinga, I. (2013). Expression of vitamin D receptor and metabolizing enzymes in multiple sclerosis-affected brain tissue. *J. Neuropathol. Exp. Neurol.* **72**, 91-105.

Sofroniew, M. V. and Vinters, H. V. (2010). Astrocytes: biology and pathology. *Acta Neuropathol.* **119**, 7-35.

Svechnikova, I., Almqvist, P. M. and Ekström, T. J. (2008). HDAC inhibitors effectively induce cell type-specific differentiation in human glioblastoma cell lines of different origin. *Int. J. Oncol.* **32**, 821-827.

Takizawa, T., Nakashima, K., Namihira, M., Ochiai, W., Uemura, A., Yanagisawa, M., Fujita, N., Nakao, M. and Taga, T. (2001). DNA methylation is a critical cell-intrinsic determinant of astrocyte differentiation in the fetal brain. *Dev. Cell* **1**, 749-758.

Tian, R., Gregor, M., Wiche, G. and Goldman, J. E. (2006). Plectin regulates the organization of glial fibrillary acidic protein in Alexander disease. *Am. J. Pathol.* **168**, 888-897.

Wahl, M. C., Will, C. L. and Lührmann, R. (2009). The spliceosome: design principles of a dynamic RNP machine. *Cell* **136**, 701-718.

Wilhelmsson, U., Li, L., Pekna, M., Berthold, C. H., Blom, S., Eliasson, C., Renner, O., Bushong, E., Ellisman, M., Morgan, T. E. et al. (2004). Absence of glial fibrillary acidic protein and vimentin prevents hypertrophy of astrocytic processes and improves post-traumatic regeneration. *J. Neurosci.* **24**, 5016-5021.

Zhou, Q., Dalgard, C. L., Wynder, C. and Doughty, M. L. (2011). Histone deacetylase inhibitors SAHA and sodium butyrate block G1-to-S cell cycle progression in neurosphere formation by adult subventricular cells. *BMC Neurosci.* **12**, 50.

Zhou, Y., Lu, Y. and Tian, W. (2012). Epigenetic features are significantly associated with alternative splicing. *BMC Genomics* **13**, 123.